

Title	Effect of mixing temperature on the carbon nanofiller distribution in immiscible blends of polycarbonate and polyolefin
Author(s)	Fan, Bowen; Wiwattananukul, Rujirek; Yamaguchi, Masayuki
Citation	European Polymer Journal, 96: 295-303
Issue Date	2017-09-19
Type	Journal Article
Text version	author
URL	http://hdl.handle.net/10119/16119
Rights	Copyright (C)2017, Elsevier. Licensed under the Creative Commons Attribution-NonCommercial-NoDerivatives 4.0 International license (CC BY-NC-ND 4.0). [http://creativecommons.org/licenses/by-nc-nd/4.0/] NOTICE: This is the author's version of a work accepted for publication by Elsevier. Bowen Fan, Rujirek Wiwattananukul, Masayuki Yamaguchi, European Polymer Journal, 96, 2017, 295-303, http://dx.doi.org/10.1016/j.eurpolymj.2017.09.021
Description	

**Effect of mixing temperature on the carbon nanofiller
distribution in immiscible blends
of polycarbonate and polyolefin**

Bowen Fan, Rujirek Wiwattananukul, and Masayuki Yamaguchi*

School of Materials Science, Japan Advanced Institute of Science and Technology

1-1 Asahidai, Nomi, Ishikawa 923-1292 JAPAN

*Corresponding author. E-mail address: m_yama@jaist.ac.jp (Masayuki Yamaguchi)

Phone: +81-761-51-1621

Fax: +81-761-51-1149

ABSTRACT

We studied the selective localization of carbon nanofillers, such as multi-walled carbon nanotube (MWCNT) and graphene nanoplatelet (GNP), in immiscible polymer blends composed of polycarbonate (PC) and polyethylene (PE) or ethylene-propylene copolymer (EPR). It was found that the distribution state of the carbon nanofillers in the composites is greatly affected by the mixing temperature and the species of nanofillers. MWCNTs resided in the PE or EPR phase in the composites, which cannot be explained by the difference in the interfacial tension. A similar morphology was detected in the PC/GNP/PE composite prepared at 300 °C. In contrast, the PC/GNP/PE composite prepared at the low temperature (250 °C) and the PC/GNP/EPR composites have the carbon nanofillers mostly in the PC phase. The selective localization in the PE or EPR phase is attributed to the surface adsorption of PE or EPR chains on the carbon nanofillers, which is more obvious for PE and at the high mixing temperature. These results demonstrate that both the species of carbon nanofillers and the mixing temperature affect the carbon nanofiller distribution in the immiscible blends.

Keywords: Polycarbonate; Polyethylene; Ethylene-Propylene Copolymer; Carbon Nanofiller; Polymer Blend

1 1. Introduction

2 Polymer composites consisting of a polymer matrix with nanofillers have
3 attracted significant interest from researchers due to their potential as
4 high-performance materials. In particular, precise control of nanofiller distribution
5 makes it possible to tune various properties of a composite of two or more polymer
6 species containing nanofillers. When nanofillers are introduced into an immiscible
7 polymer blend composed of two polymer species, three cases of filler dispersion can
8 take place: (i) nanofillers are randomly dispersed in both polymer phases, (ii)
9 nanofillers are unevenly distributed in each phase, and (iii) nanofillers localize at the
10 boundary of phases [1-4]. In order to control the structure, the recipe of a polymer
11 blend and processing conditions have to be appropriately selected.

12 Dispersing nanofillers uniformly in an immiscible polymer blend is difficult even
13 with stress that surpasses a cohesive force of filler agglomerations. Moreover, in many
14 cases uneven distribution occurs. The main factors affecting localization of nanofillers
15 are classified into thermodynamic and kinetic effects [5]. The thermodynamic effect is
16 determined by the difference in the interfacial tension among polymer pairs and filler
17 [6-8]. According to Mamunya, the spatial distribution of carbon black (CB) in an
18 immiscible polymer blend is determined by the interfacial tension Γ_{i-c} between
19 i -polymer and CB, as well as the interfacial tension between polymer pairs Γ_{A-B} [9].
20 This behavior is well expressed using the wetting coefficient ω_a defined as equation
21 (1) [1], which was confirmed by previous researches [10-12];

$$22 \quad \omega_a = \frac{\Gamma_{A-filler} - \Gamma_{B-filler}}{\Gamma_{A-B}} \quad (1)$$

23 when ω_a is smaller than -1, fillers exist in phase A. In contrast, fillers exist in phase
24 B at $\omega_a > 1$. Moreover, fillers are localized at the phase boundary at $-1 < \omega_a < 1$.

25 Kinetic effect [13] can be controlled by the mixing process. It has been
26 demonstrated that the distribution state of fillers in a polymer blend is often different
27 from the equilibrium state because of its high viscosity. In particular, nanofillers can
28 not diffuse into a polymer with an extremely high viscosity [14,15]. In this case,
29 nanofillers have to reside in a low viscous phase or on the surface of a high viscous

30 phase. Such localization leads to an electrical conductive path with a small amount of
31 conductive fillers [16-19].

32 In the previous paper [20], we found that multi-walled carbon nanotubes
33 (MWCNTs) were dispersed in the continuous polypropylene (PP) phase in the blends
34 of PP and ethylene-propylene copolymer (EPR) when the composite was prepared at
35 low temperatures. Furthermore, nitrogen gas purging was effective to the preferential
36 distribution of MWCNTs in the matrix, i.e., PP. Without the use of nitrogen, in
37 contrast, more MWCNTs were distributed in the dispersed EPR phase when the
38 mixing temperature was high, e.g., 280 °C. This is attributed to the adsorption of EPR
39 molecules on the MWCNT surface during melt mixing. These results significant for
40 the material design of rubber-toughened plastics, although it is still unknown whether
41 nanofiller distribution is controlled by the mixing condition for other blend systems.

42 In this research, we investigated the effect of the mixing conditions, specifically
43 temperature, on the nanofiller localization using immiscible blends composed of
44 polycarbonate (PC) and polyethylene (PE) or EPR. The effect of shape and species of
45 carbon nanofillers on the distribution state was studied using MWCNT and graphene
46 nanoplatelet (GNP).

47

48 **2. Experimental**

49 *2.1 Materials*

50 The polymers used in this study were commercially available bisphenol A
51 polycarbonate (PC) (Panlite L-1225Y, Teijin, Japan, MFR=11 [g/10 min]),
52 high-density polyethylene (PE) (HJ590N, Japan Polyethylene, MFR=40 [g/10 min]),
53 and ethylene-propylene copolymer (EPR) (EP11, JSR, Japan) with an ethylene
54 content of 52 wt.%. The Mooney viscosity $ML_{(1+4)}$ 100 °C of EPR is 40. Because of
55 the large amount of propylene, the EPR is fully amorphous at room temperature. The
56 number- and weight-average molecular weights, characterized by a size exclusion
57 chromatograph (SEC) (HLC-8020, Tosoh, Japan) using chloroform as an eluent, are
58 $M_n = 1.9 \times 10^4$ and $M_w = 9.7 \times 10^4$ for PC and 4.0×10^6 and 4.7×10^6 for EPR, as a
59 polystyrene standard. Moreover, M_n and M_w of PE were also characterized by SEC

60 using 1,2,4-trichlorobenzene at 140 °C and found to be 8.7×10^3 and 4.9×10^4 ,
61 respectively, as a polyethylene standard. The density of PE is 960 [kg/m³] at room
62 temperature.

63 Multi-walled carbon nanotubes (MWCNTs) were produced by a catalytic
64 chemical vapor deposition method using a floating reactant method and subsequent
65 thermal treatment up to 2600 °C. Typical diameters of the MWCNTs range from 40 to
66 80 nm, while the lengths are between 10 and 20 μm. The density is approximately
67 2300 [kg/m³]. PC/MWCNT (80/20, in weight fraction) was provided by Hodogaya
68 Chemical (Japan) in pellet form. Graphene nanoplatelets (GNPs) were produced by
69 Graphene Platform in powder form. The average diameter ranges from 3 to 30 μm,
70 and the thickness is between 0.3 and 1.5 nm. PC/GNP (80/20, in weight ratio) was
71 prepared by adding the GNP powder to the PC-chloroform solution at room
72 temperature. After drying, the composite was kneaded at 280 °C for 15 min using a
73 co-rotating twin-screw mixer with a disclosed condition
74 (ULT15TWNANO-15MG-NH, Technovel, Japan). The screw rotation speed was 250
75 rpm.

77 2.2 Sample preparation

78 Prior to melt blending, PC/MWCNT (80/20) and PC/GNP (80/20) were dried at
79 120 °C for 8 h in a vacuum oven in order to remove the moisture. PC/Nanofiller
80 (80/20) and PE or EPR were mixed using a 30cc internal batch mixer (IMC-1891,
81 Imoto, Japan) at various temperatures for 20 min with a blade rotation speed of 50
82 rpm. The blend ratio of PC/Nanofiller (80/20) to PE or EPR was 50/50 in the weight
83 fraction, i.e., PC/Nanofiller/PE or EPR (40/10/50) with 10000 ppm of a thermal
84 stabilizer (Sumilizer-GP, Sumitomo Chemical, Japan). In addition, PC/PE (40/50, in
85 weight ratio) and PC/EPR (40/50, in weight ratio) were also prepared as reference
86 samples under the same condition, but without carbon nanofillers.

87 The obtained samples were compressed into flat sheets with a thickness of 1 mm
88 using a laboratory compression-molding machine at 250 °C under 10 MPa for 3 min
89 and subsequently cooled at 25 °C for 3 min.

90

91 *2.3 Measurements*

92 Flat sheets of PC/PE, PC/MWCNT/PE, and PC/GNP/PE with a thickness of
93 about 1 mm were immersed in chloroform to eliminate PC fraction at room
94 temperature for one day. Then, the insoluble portion in chloroform, which was
95 collected by using a paper filter with 110 μm of a pore size, was further immersed into
96 hot-xylene at 140 $^{\circ}\text{C}$ for 6 h. Prior to the measurements, it was confirmed that PE is
97 fully dissolved in hot-xylene under the same condition. The chloroform and xylene
98 solutions containing dissolved polymers were collected and dried to characterize the
99 polymer species. Another immersion experiment was performed using
100 dichloromethane at room temperature for three days using the blend and composites
101 comprising EPR, because dichloromethane selectively dissolves the PC fraction.
102 Moreover, the insoluble portion collected by the paper filter was dried and weighed to
103 calculate the soluble fraction.

104 Thermal properties were evaluated using a differential scanning calorimeter
105 (DSC) (DSC 8500, Perkin Elmer, USA) under nitrogen atmosphere. The sample was
106 heated from room temperature to 200 $^{\circ}\text{C}$ at a scanning rate of 10 $^{\circ}\text{C}/\text{min}$ to evaluate
107 the crystallinity and the melting point T_m . After keeping at 200 $^{\circ}\text{C}$ for 3 min, the
108 sample was cooled to 30 $^{\circ}\text{C}$ at 10 $^{\circ}\text{C}/\text{min}$ to evaluate the crystallization temperature
109 T_c .

110 The morphology and localization of carbon nanofillers in the composites were
111 detected using a scanning electron microscope (SEM) (S4100, Hitachi, Japan). For
112 SEM observations, the sheets were cryofractured in liquid nitrogen. Furthermore, the
113 detail characterization was performed to obtain backscattered electron images using a
114 field-emission SEM (JSM-7100F, JEOL, Japan). The sheets were cut by an
115 ultra-microtome (MT-XL, RMC-Boeckeler, AZ, USA) at -100 $^{\circ}\text{C}$ and stained by
116 ruthenium tetroxide prior to the observation.

117 The frequency dependence of the dynamic tensile modulus was measured using a
118 dynamic mechanical analyzer (Rheogel-E4000, UBM, Japan) from 0.1 to 100 Hz at
119 room temperature. Rectangular specimens with 1 mm thickness were cut from the

120 compressed films.

121 Electrical resistivity measurements were carried out on the surface of the
 122 compressed films using a constant-current supply resistivity meter (MCP-T610,
 123 Mitsubishi Chemical Analytech, Japan). The resistivity was measured five times for
 124 each sample at room temperature and the average value was calculated.

125

126 3. Results and discussion

127 3.1 PC/PE with carbon nanofillers

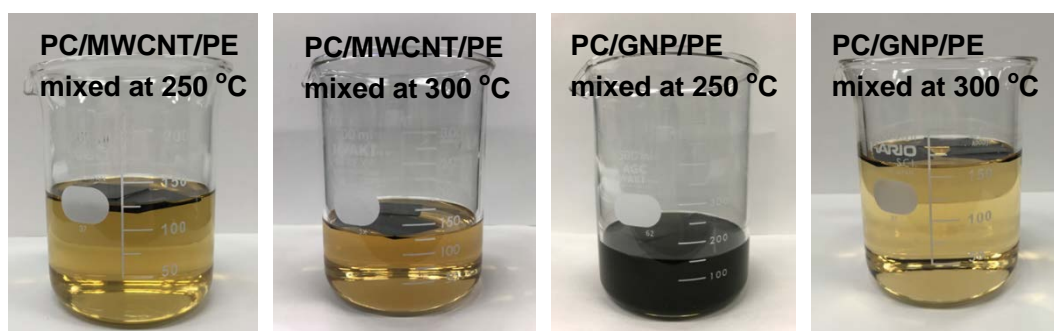
128 Immersion experiments were carried out to reveal the nanofiller distribution as
 129 shown in Figure 1. The weight fraction of the dissolved sample was measured after
 130 drying and confirmed to be identical to the PC fraction, i.e., 40 wt.% in the
 131 PC/MWCNT/PE composites, as shown in Table 1. Furthermore, the FT-IR spectra,
 132 shown in Figure 2, demonstrate that only PC was dissolved into the solvent. Although
 133 the spectra for the soluble part in the composites prepared at 300 °C are shown in the
 134 figure, similar results were obtained for the composites mixed at 250 °C.

135

136 **Table 1** Weight fraction of PC/PE with carbon nanofillers evaluated by the immersion
 137 experiment.

Filler	Mixing Temperature	Soluble part in CHCl ₃ (wt.%)	Insoluble part in CHCl ₃	
			Soluble part in xylene (wt.%)	Insoluble part in xylene (wt.%)
MWCNT	250 °C	39	46	15
	300 °C	39	47	14
GNP	250 °C	42	48	11
	300 °C	39	50	11

138



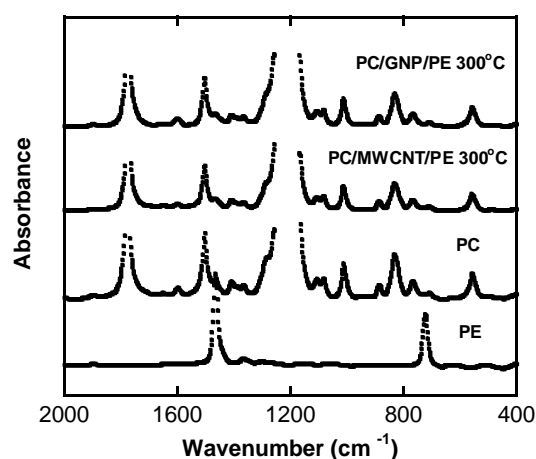
139

140 **Fig. 1.** Photographs of the immersion experiment in chloroform.

141

142 As seen in the photographs, the solutions were yellow, not black, for the
143 PC/MWCNT/PE composites, irrespective of the mixing temperature, although most
144 PC was dissolved into chloroform. This result suggests that most MWCNTs
145 transferred from PC to PE during mixing, which is attributed to the surface adsorption
146 of PE chains on the surface of the MWCNTs, as explained in detail later. The same
147 result was obtained for the PC/GNP/PE (40/10/50) composite prepared at 300 °C. In
148 contrast, the solution of PC/GNP/PE (40/10/50) composite prepared at 250 °C became
149 black, indicating that a large amount of GNPs still remained in the PC phase.

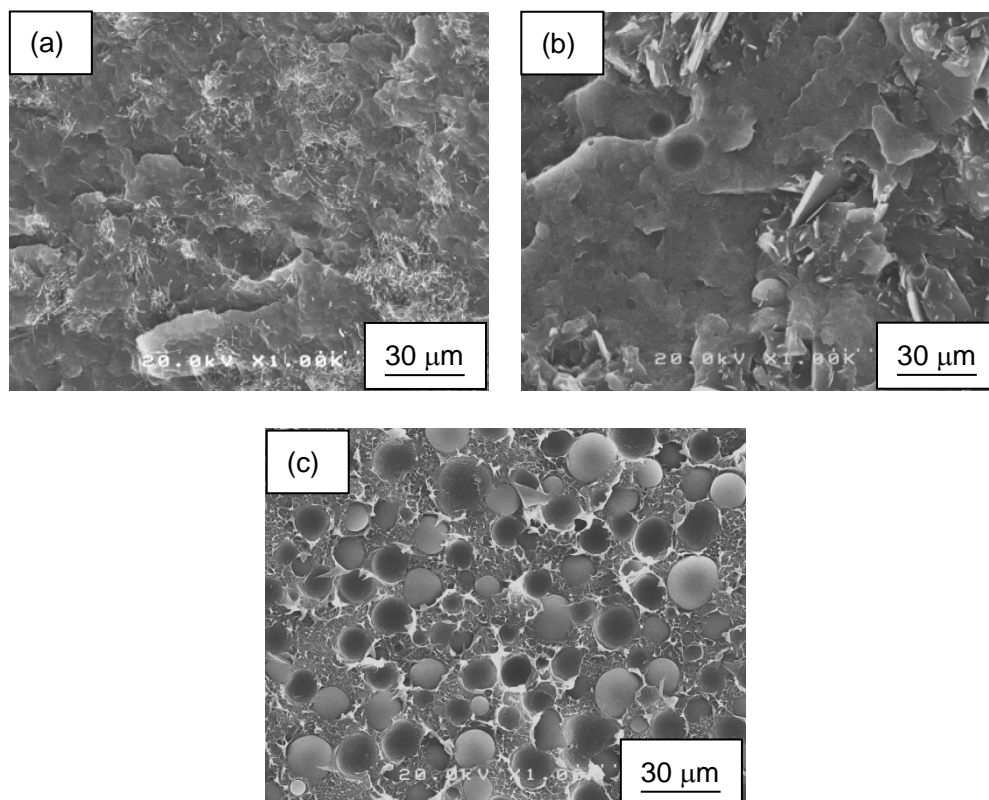
150



151

152 **Fig. 2.** Infrared spectra of the soluble part in chloroform at room temperature for
153 PC/MWCNT/PE (40/10/50) and PC/GNP/PE (40/10/50) prepared at 300 °C. The
154 spectra of pure PC and PE are also shown as references.

155



156

157

158 **Fig. 3.** SEM images of cryofractured surface of (a) PC/MWCNT/PE (40/10/50), (b)
159 PC/GNP/PE (40/10/50), and (c) PC/PE (40/50). All samples were mixed at 300 °C.

160

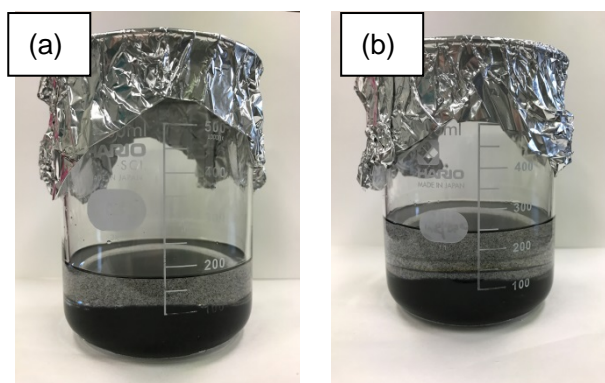
161 Cryofractured surface of the composites prepared at 300 °C was observed by
162 SEM. As shown in Figures 3 (a) and (b), the carbon nanofillers were unevenly
163 distributed only in a specific area, and some areas did not have any nanofillers.
164 Considering that the solution color was fairly transparent, the area with carbon
165 nanofillers was determined to be the PE phase.

166 To characterize the PE phase, the insoluble portion in chloroform was put into
167 boiled xylene. It was found that the insoluble portion was detected even in the hot
168 xylene for the PC/MWCNT/PE composites, demonstrating that trace amounts of PE
169 fraction are strongly adsorbed on the MWCNT surface and form network structure.
170 Furthermore, the solution was transparent as shown in Figure 4. The weight fraction
171 of the remaining insoluble part in the hot xylene is shown in Table 1. The dissolved
172 part in hot xylene (46.6 wt.% of the PC/MWCNT/PE prepared at 300 °C) was found
173 to be PE by FT-IR and DSC. The surface of the insoluble portion in hot xylene is

174 displayed in Figure 5. PE crystals, confirmed by the DSC measurement (Fig. 6), were
175 clearly detected on the MWCNT surface even after immersion in hot xylene.

176 The surface modification of MWCNTs by PE molecules enhances the selective
177 localization of MWCNTs in the PE phase. This is a similar effect of the bound rubber
178 molecules in immiscible rubber blends [21].

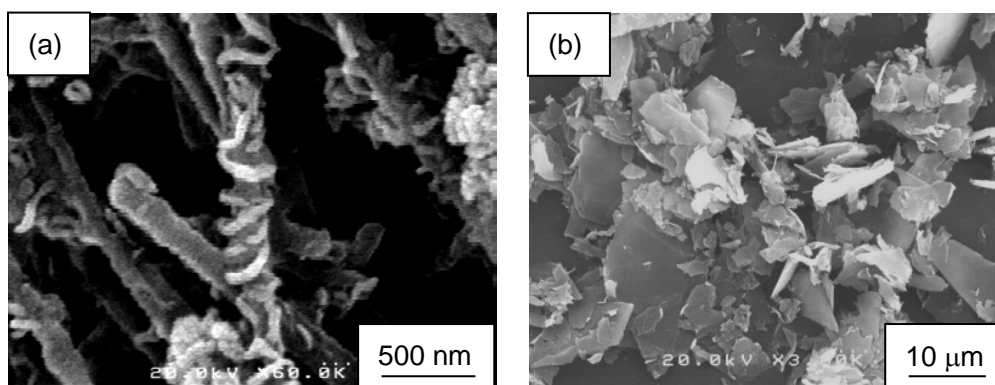
179



180

181 **Fig. 4.** Photographs of the immersion experiments in hot xylene using the insoluble
182 part in chloroform. (a) PC/MWCNT/PE and (b) PC/GNP/PE mixed at 300 °C.

183



184

185 **Fig. 5.** SEM images of the surface of the insoluble part in hot xylene. (a)
186 PC/MWCNT/PE and (b) PC/GNP/PE mixed at 300 °C.

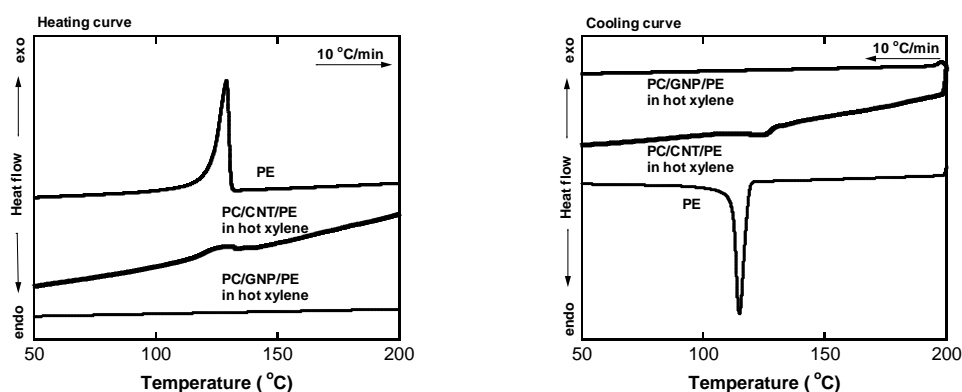
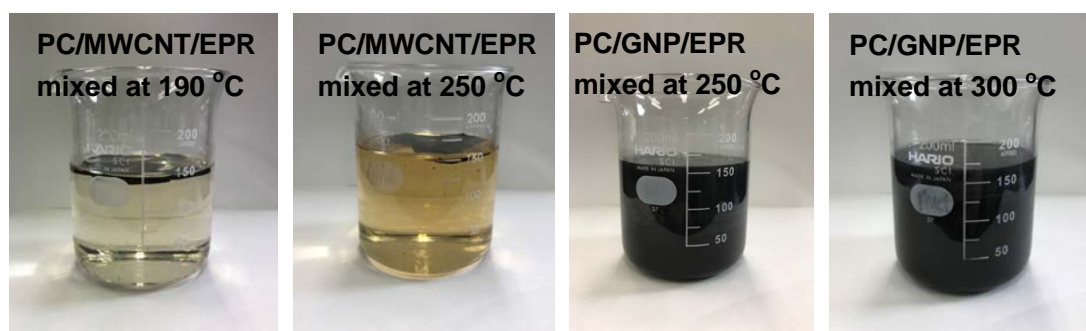


Fig. 6. DSC heating and cooling curves for the insoluble part in hot xylene.

GNPs were dispersed in hot xylene even for the composite prepared at 300 °C, suggesting that network structure composed of PE molecules and GNPs was not well developed in the composite. The dispersed GNPs in the hot xylene were collected and observed by SEM after drying. PE crystals were not clearly detected on the GNP surface. Moreover, the melting and crystallization peaks ascribed to PE were not detected by the DSC measurements as shown in Figure 6. Although there is a possibility that the adsorbed PE shows low crystallinity, the amount of the insoluble PE (weight fraction of insoluble part in xylene – weight fraction of carbon nanofillers (10 wt.)) is significantly low as shown in Table 1. In the case of the composite with MWCNTs, the nucleating ability to PE was confirmed from the DSC cooling curve. These results suggest that the surface of MWCNTs is more active than that of GNPs. Presumably, the surface activity of carbon nanofillers is affected by surface defects and/or oxidized functions.

3.2 PC/EPR with carbon nanofillers

Similar experiments were performed using EPR instead of PE. Figure 7 shows the photographs of the solvent immersion experiments. Dichloromethane was used as a solvent for the composites of PC/EPR, because it dissolves PC, not EPR at room temperature, which was confirmed prior to the experiments.



210

211 **Fig. 7.** Photographs of the immersion experiments in dichloromethane.

212

213 The solutions for the PC/MWCNT/EPR composites were fairly transparent.

214 Considering the weight fraction of the insoluble portion (Table 2) and the FT-IR

215 spectra of the soluble part (Fig. 8), most MWCNTs moved from PC to EPR during

216 mixing even at 190 °C. In contrast, the solutions of the PC/GNP/EPR composites

217 were black irrespective of the mixing temperature, suggesting that GNPs remained in

218 the PC phase. The result demonstrates that the species of carbon nanofillers greatly

219 affects the transfer phenomenon; i.e., The adhesion on the GNP surface of EPR

220 molecules is significantly different from that of PE. In other words, GNPs prefer to

221 stay in PE rather than EPR. It is well known that polyolefins show the autoxidation

222 reaction at mixing/processing operations [22-28]. The free radical generation becomes

223 prominent at high temperatures especially beyond 250 °C [24-30]. Although PE shows

224 crosslinking reaction at conventional processing temperature, polypropylene (PP)

225 exhibits chain scission reaction. The difference stems from the existence of tertiary

226 carbon atoms in the backbone. Therefore, PP shows β -cleavage of tertiary alkyl

227 radicals, which easily occurs, leading to decrease in molecular weight. In contrast,

228 relatively stable radicals involving peroxide radicals in ethylene unit play an

229 important role on the chemical reaction with the surface active site of carbon

230 nanofillers during mixing. Moreover, the recent studies indicated that the MWCNTs

231 accelerate the radical generation for PE and EPR at high temperatures, e.g., 250 –

232 300 °C [20,30]. The present experimental results also support the mechanism that free

233 radicals in ethylene unit, generated at high temperature, are responsible for the

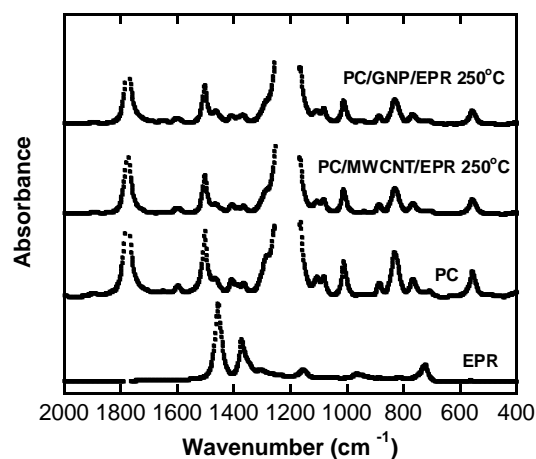
234 reaction with surface of carbon nanofillers.

235 Table 2 shows that the insoluble portion of the composite with MWCNTs is less
 236 than that of the composites with GNPs. Moreover, the weight fraction is lower than 60
 237 wt.%, i.e., the sum of the weight fractions of EPR and carbon fillers. This result
 238 indicates that some EPR molecules, which may be degraded by chain scission reaction,
 239 dissolve into the solvent.

240

241 **Table 2** Weight fraction of PC/EPR with carbon nanofillers evaluated by the
 242 immersion experiment.

Filler	Mixing Temperature	Insoluble part in CH ₂ Cl ₂ (wt.%)
MWCNT	190 °C	55
	250 °C	54
GNP	250 °C	56
	300 °C	57



243

244 **Fig. 8.** Infrared spectra of the soluble parts in dichloromethane at room temperature
 245 for PC/MWCNT/EPR (40/10/50) and PC/GNP/EPR (40/10/50).

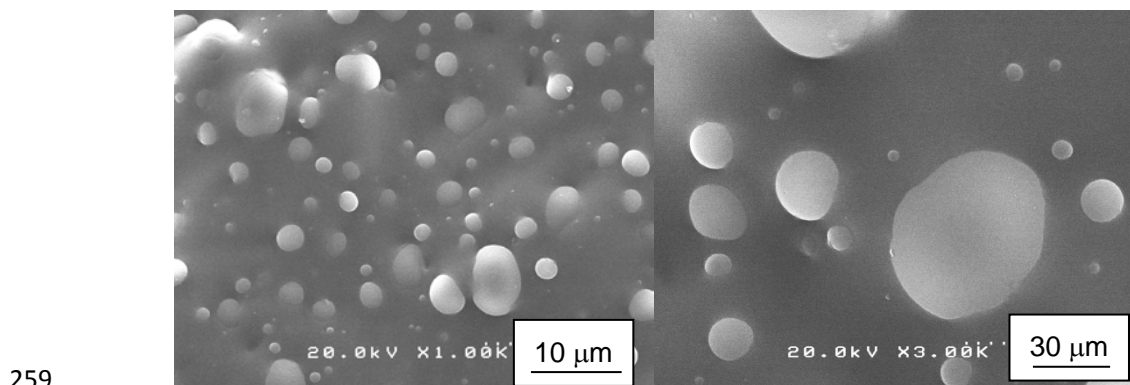
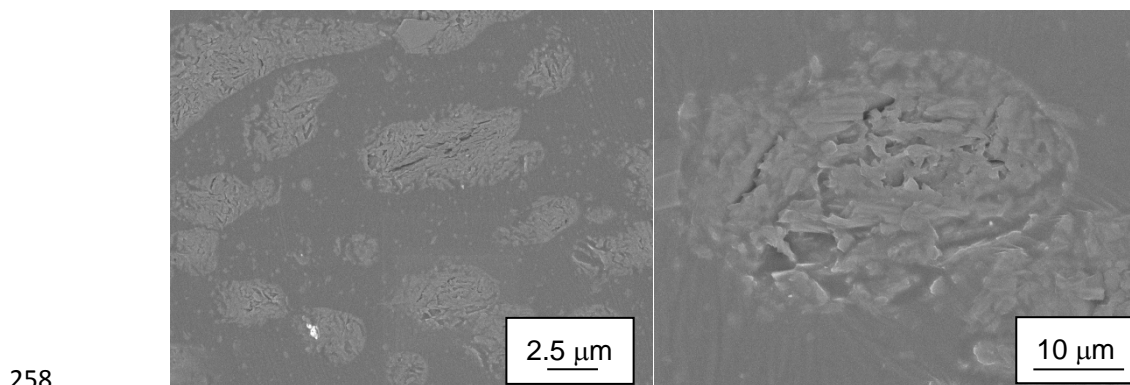
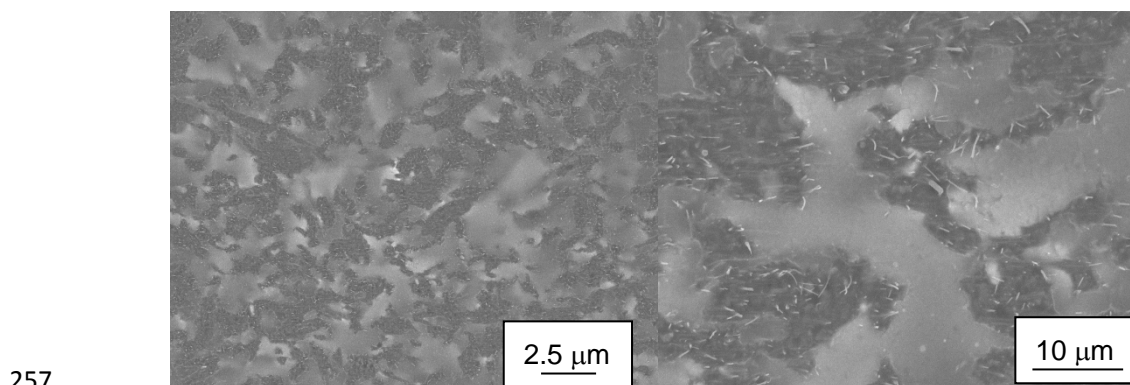
246

247 The solution was filtrated to remove GNPs by the paper filter to confirm the
 248 polymer species by FT-IR after drying. The spectra were the almost the same with that
 249 of the pure PC. The EPR fraction was not detected at least by the FT-IR measurements.

250 After the solvent immersion experiment, a chunk of the sample was detected in the
251 solution. This result indicates that EPR is a matrix of the composites.

252 The cut surface of the composites, i.e., PC/MWCNT/EPR and PC/GNP/EPR,
253 was observed by backscattered electron image of SEM to confirm the distribution
254 state of the nanofillers clearly. The surface cut by the ultramicrotome was observed
255 after the exposure to the vapor of ruthenium tetroxide.

256



260 **Fig. 9.** SEM images (top) cut surface of PC/MWCNT/EPR (40/10/50), (middle) cut
261 surface of PC/GNP/EPR (40/10/50), and (bottom) cryogenically fractured surface of
262 PC/EPR (40/50). All samples were prepared at 250 °C.

263

264 As shown in Figure 9, the phase-separated structure was clearly detected for both
 265 composites, although their nanofiller distribution was greatly differed. The nanofillers
 266 existed in one of the co-continuous phases, i.e., EPR, in the composite with MWCNTs.
 267 In contrast, sea-island structure was observed for the composite with GNPs, in which
 268 GNPs were selectively localized in the dispersed phase. The phase boundary of the
 269 composite with MWCNTs was not smooth, which must be due to the high viscosity of
 270 the continuous phase, leading to the long characteristic time of orientation relaxation.

271 The surface resistivity was shown in Table 3. The resistivity must correspond
 272 with the structure and localization state of the nanofillers. In other words, the
 273 composite with low surface resistivity contains a large amount of nanofillers in the
 274 continuous phase. For example, the PC/MWCNT/EPR prepared at 250 °C showed low
 275 resistivity, whereas PC/GNP/EPR prepared at the same temperature exhibited high
 276 resistivity. This is reasonable because the former has MWCNTs in the continuous
 277 phase while the latter has GNPs in the dispersed phase as demonstrated in Fig. 9.

278

279

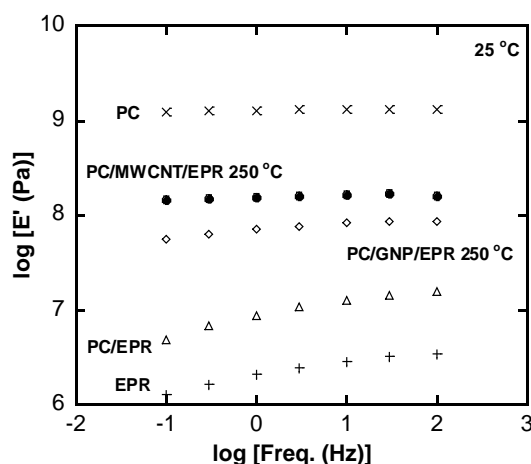
Table 3 Surface Resistivity

Polymer pair	Filler	Mixing Temperature	Surface Resistivity $\Omega/\text{sq.}$
PC/PE	MWCNT	250 °C	3.3×10^5
		300 °C	1.5×10^2
	GNP	250 °C	1.9×10^9
		300 °C	7.8×10^9
PC/EPR	MWCNT	190 °C	4.1×10^8
		250 °C	9.2×10^3
	GNP	250 °C	2.8×10^{12}
		300 °C	4.5×10^{13}

280

281 The dynamic tensile modulus at room temperature was measured using the films
 282 of PC/nanofiller/EPR composites and the reference samples as a function of frequency

283 as shown in Figure 10.



284

285 **Fig. 10.** Frequency dependence of tensile storage modulus E' for PC, EPR, PC/EPR
 286 (40/50), PC/MWCNT/EPR (40/10/50), and PC/GNP/EPR (40/10/50) at room
 287 temperature.

288

289 Because PC is in the glassy region at this temperature, it shows a constant value
 290 of the tensile storage modulus E' in a wide range of frequencies. The
 291 PC/MWCNT/EPR composite prepared at 250 °C also shows a constant E' . This result
 292 indicates that PC is a continuous phase, which corresponds with the SEM image. In
 293 contrast, E' of EPR is a typical value in the rubber region and is frequency dependent.
 294 The frequency dependence of E' is also detected for PC/EPR, and the PC/GNP/EPR
 295 composite prepared at 250 °C. The result is reasonable because the EPR phase exists
 296 as a continuous phase as shown in Fig.9. As a result, E' of the PC/MWCNT/EPR
 297 composite is significantly higher than that of the PC/GNP/EPR composite.

298

299 4. Conclusion

300 The interphase transfer of carbon nanofillers in the immiscible blends such as
 301 PC/PE and PC/EPR was studied. Although the nanofiller distribution in an immiscible
 302 polymer blend can be predicted by the wetting coefficient in general, which can be
 303 expressed by the interfacial tensions among components, the adsorption of PE and

304 EPR molecules on the carbon surface, i.e., bound molecules, greatly affects the
305 distribution state. It was found that PE molecules adsorb more easily on the carbon
306 nanofillers than EPR, suggesting that ethylene unit is responsible for the surface
307 adsorption. Furthermore, the surface adsorption was accelerated by high temperature
308 mixing, presumably owing to the frequent radical generation. Finally, the surface of
309 MWCNT is found to be more active than that of GNP used in this study. These results
310 demonstrate that bound molecules that are generated during mixing play an important
311 role on the nanofiller distribution.

312

313 **Acknowledgments**

314 This work was promoted by COI program “Construction of next-generation
315 infrastructure system using innovative materials” – Realization of safe and secure
316 society that can coexist with the Earth for centuries – Supported by Japan Science and
317 Technology Agency (JST). The authors also would like to express their gratitude to
318 Hodogaya Chemical Co., Ltd. for their valuable advice and the kind supply of the
319 samples employed in this study. The authors appreciate TOSOH Analysis and
320 Research Center Co., LTD for their technical support of SEM observation.

321

322 Reference

- 323 [1] Sumita M, Sakata K, Asai S, Miyasaka K, Nakagawa H. Dispersion of fillers and
324 the electrical conductivity of polymer blends filled with carbon black. *Polym Bull*
325 1991;25:265-71.
- 326 [2] Mamunya YPJ. Morphology and percolation conductivity of polymer blends
327 containing carbon black. *J Macromol Sci Part B Phys* 1999;38:615-22.
- 328 [3] Ray SS, Pouliot S, Bousmina M, Utracki LA. Role of organically modified layered
329 silicate as an active interfacial modifier in immiscible polystyrene/polypropylene
330 blends. *Polymer* 2004;45:8403-13.
- 331 [4] Yoon H, Okamoto K, Yamaguchi M. Carbon nanotube imprinting on a polymer
332 surface. *Carbon* 2009;47:2840-6.
- 333 [5] Wu S. *Polymer Interface and Adhesion*, Marcel Dekker, 1982.
- 334 [6] Gubbels F, Jérôme R, Vanlathem E, Deltour R, Blacher S, Brouers F. Kinetic and
335 thermodynamic control of the selective localization of carbon black at the
336 interface of immiscible polymer blends. *Chem Mater* 1998;10:1227-35.
- 337 [7] Wu S. Interfacial and surface tensions of polymers. *J Macromol Sci Rev*
338 *Macromol Chem* 1974;10:1-73.
- 339 [8] Owens DK, Wendt RC. Estimation of the surface free energy of polymers. *J Appl*
340 *Polym Sci* 1969;13:1741-7.
- 341 [9] Mamunya YP. Morphology and percolation conductivity of polymer blends
342 containing carbon black. *J Macromol Sci Phys* 1999;38:615-22.
- 343 [10] Gubbels F, Jérôme R, Teyssié P, Vanlathem E, Deltour R, Calderone A, Brédas JL.
344 Selective localization of carbon black in immiscible polymer blends: a useful tool
345 to design electrical conductive composites. *Macromolecules* 1994;27:1972-4.
- 346 [11] Ross S, Morrison ED. *Colloidal Systems and Interfaces*, Wiley, New York, 1988.
- 347 [12] Sumita M, Sakata K, Asai S, Miyasaka K, Nakagawa H. Dispersion of fillers and
348 the electrical conductivity of polymer blends filled with carbon black. *Polym Bull*
349 1991;25:265-71.
- 350 [13] Gubbels F, Blacher S, Vanlathem E, Jerome R, Deltour R, Brouers F, Teyssie P.
351 **Design of electrical conductive composites: Key role of the morphology on the**

- 352 electrical properties of carbon black filled polymer blends. 1995;28:1559-66.
- 353 [14] Zaikin AE, Zharinova EA, Bikmullin RS. Specifics of localization of carbon
354 black at the interface between polymeric phases. *Polym Sci Ser A*
355 2007;49:328-36.
- 356 [15] Lisunova MO, Mamunya YP, Lebovka NI, Melezhyk AV. Percolation behaviour
357 of ultrahigh molecular weight polyethylene/multi-walled carbon nanotubes
358 composites. *Eur Polym J* 2007;43:949-58.
- 359 [16] Zaikin AE, Karimov RR, Arkhireev VP. A study of the redistribution conditions
360 of carbon black particles from the bulk to the interface in heterogeneous polymer
361 blends. *Colloid J* 2001;63:53-9.
- 362 [17] Feng J, Chan CM, Li JX. A method to control the dispersion of carbon black in
363 an immiscible polymer blend. *Polym Eng Sci* 2003;43:1058-63.
- 364 [18] Liebscher M, Tzounis L, Pötschke P, Heinrich G. Influence of the viscosity ratio
365 in PC/SAN blends filled with MWCNTs on the morphological, electrical, and
366 melt rheological properties. *Polymer* 2013;54:6801-8.
- 367 [19] Clarke J, Clarke B, Freakley PK, Sutherland I. Compatibilising effect of carbon
368 black on morphology of NR–NBR blends. *Plastics, Rubber and Composites*
369 2001;30:39-44.
- 370 [20] Wiwattananukul R, Fan B, Yamaguchi M. Improvement of rigidity for
371 rubber-toughened polypropylene via localization of carbon nanotubes. *Compos*
372 *Sci Technol* 2017;141:106-12
- 373 [21] Datta S. Elastomer blends, in *Polymer blends*. Eds. Paul DR, Bucknall CB. Wiley,
374 2000.
- 375 [22] Schnabel W. *Polymer degradation*. Hanser, 1981.
- 376 [23] Hawkins WL. *Polymer degradation and stabilization*. Springer, 1984.
- 377 [24] Peacock AJ. *Handbook of polyethylene*. Marcel Dekker, 2000.
- 378 [25] Kuroki T, Sawaguchi T, Niikuni S, Ikemura T. Mechanism for long chain
379 branching in the thermal degradation of linear high-density polyethylene.
380 *Macromolecules* 1982;15:1460-4.
- 381 [26] Andersson T, Stalborm B, Wesslen B. *Degradation of polyethylene during*

-
- 382 extrusion II: Degradation of low-density polyethylene and high-density
383 polyethylene in film extrusion. *J Appl Polym Sci* 2004;91:1525-37.
- 384 [27] Al-Malaika S, Peng X, Watson H. Metallocene ethylene-1-octene copolymers:
385 Influence of comonomer content on thermos-mechanical, rheological, and
386 thermos-oxidative behaviors before and after melt processing in an internal mixer.
387 *Polym Degrad Stab* 2006;91:3131-48.
- 388 [28] Ono K, Yamaguchi M. Thermal and mechanical modification of LDPE in
389 single-screw extruder. *J Appl Polym Sci* 2009;113:1462-70.
- 390 [29] Siriprumponthum M, Nobukawa S, Satoh Y, Sasaki H, Yamaguchi M. Effect of
391 thermal modification on rheological properties of polyethylene blends. *J Rheology*
392 2014;58:449-65.
- 393 [30] Wiwattananukul R, Hachiya Y, Endo T, Nobukawa S, Yamaguchi M. Anomalous
394 transfer phenomenon of carbon nanotube in the blend of polyethylene and
395 polycarbonate. *Comp Part B* 2015;78:409-14.